DENTAL MATERIALS 35 (2019) 1532–1544

Available online at www.sciencedirect.com

ScienceDirect

journal homepage: www.intl.elsevierhealth.com/journals/dema

Synthesis of chemically modified BisGMA analog with low viscosity and potential physical and biological properties for dental resin composite

Abdel-Basit Al-Odayni[a], *Randa Alfotawi*[b], *Rawaiz Khan*[c], *Waseem Sharaf Saeed*[a], *Abdullah Al-Kahtani*[a], *Taieb Aouak*[a], *Ali Alrahlah*[c,d,*]

[a] *Chemistry Department, College of Science, King Saud University, P.O. Box 2455, Riyadh 11451, Saudi Arabia*
[b] *Maxillofacial Surgery Department, College of Dentistry, King Saud University, Riyadh 11545, Saudi Arabia*
[c] *Engineer Abdullah Bugshan Research Chair for Dental and Oral Rehabilitation, College of Dentistry, King Saud University, Riyadh 11545, Saudi Arabia*
[d] *Restorative Dental Sciences Department, College of Dentistry, King Saud University, Riyadh 11545, Saudi Arabia*

ARTICLE INFO

Article history:
Received 17 February 2019
Received in revised form
11 June 2019
Accepted 16 July 2019

Keywords:
Dental material
BisGMA derivative
Dental resin composite
Low viscosity
Cytotoxicity

ABSTRACT

Objectives. The currently available commercial dental resin composites have limitations in use owing to the high viscosity and water sorption of Bisphenol A glycidyl methacrylate (BisGMA). The objective of this study was to obtain a BisGMA analog with reduced viscosity and hydrophilicity for potential use as an alternative to BisGMA in dental resin composites.
Methods. The targeted chlorinated BisGMA (Cl-BisGMA) monomer was synthesized via the Appel reaction. The structural modification was confirmed via ^{1}H- and ^{13}C nuclear magnetic resonance spectroscopy, Fourier transform infrared spectroscopy, and mass spectrometry. Five resin mixtures (70:30 wt.%: F1 = BisGMA/TEGDMA; F2 = Cl-BisGMA/TEGDMA; F3 = Cl-BisGMA only; F4 = Cl-BisGMA/BisGMA; F5 contained 15% TEGDMA with equal amounts of BisGMA and Cl-BisGMA) were prepared. The viscosity, degree of double-bond conversion (DC), water sorption (W_{SP}), and solubility (W_{SL}) were tested. Cell viability and live/dead assays, as well as cell attachment and morphology assessments, were applied for cytotoxicity evaluation.
Results. Cl-BisGMA was successfully synthesized with the viscosity reduced to 7.22 (Pa s) compared to BisGMA (909.93, Pa s). Interestingly, the DC of the F2 resin was the highest (70.6%). By the addition of equivalence concentration of Cl-BisGMA instead of BisGMA, the W_{SP} was decreased from 2.95% (F1) to 0.41% (F2) with no significant change in W_{SL}. However, the W_{SL} increased with high Cl-BisGMA content. Biological tests revealed that all the resins were biocompatible during CL1 incubation.
Significance. The experimental resins based on Cl-BisGMA exhibited improved properties compared with the control samples, e.g., biocompatibility and lower viscosity, indicating that Cl-BisGMA can be considered as a potential monomer for application in dental resin composites.

* *Corresponding author at*: Department of Restorative Dental Sciences, College of Dentistry, King Saud University, Riyadh 11545, Saudi Arabia.
E-mail address: aalrahlah@ksu.edu.sa (A. Alrahlah).
https://doi.org/10.1016/j.dental.2019.07.013

1. Introduction

Dental cavities are commonly filled by using four types of restorative dental materials: metals, ceramics, polymers, and composites [1]. However, owing to their ease of handling [2,3] and superior aesthetic characteristics [4,5], light-cured polymer composites are widely used for dental rehabilitation. Generally, these dental resin composites consist of three key components: (i) a mixture of dimethacrylate monomers (Bisphenol A glycidyl methacrylate (BisGMA), triethylene glycol dimethacrylate (TEGDMA), and urethane dimethacrylate), which form the resin network upon polymerization; (ii) reinforcing filler particles (silica, zirconia, titanium oxide, barium silicate glass, etc.); and (iii) a polymerization initiating system (e.g., camphorquinone (CQ)) [6,7]. The polymerization mechanism, handling characteristics, and application performance of these composites are closely related to the selection of the monomers.

BisGMA is the most widely used monomer in the preparation of dental restorative composite resins [8–11]. Under visible light, BisGMA rapidly polymerizes owing to the existence of a light-sensitive free-radical initiator, e.g., CQ, leading to a hard crosslinked network structure resembling a natural tooth. Thus, BisGMA is a material of choice for dental restorative applications [12,13]. However, the presence of two secondary hydroxyl groups and π–π interactions due to the aromatic rings result in a high initial viscosity (molecular weight (MW) = 512.6 g/mol, $\eta = \tilde{1}200$ Pa s) of the monomer; thus, the homopolymer usually does not reach high conversion [14]. Furthermore, the strong intramolecular hydrogen bonding reduces the reactivity and mobility of the monomer during the polymerization process and causes hydrophilicity in the resulting composite resin [15]. To reduce the viscosity, improve the handling properties of the monomer mixture, and allow incorporation of higher inorganic filler contents, BisGMA is generally combined with TEGDMA (MW = 286.3 g/mol, $\eta = \tilde{0}.01$ Pa s) [11,16]. However, owing to its linear molecular structure and the triethylene oxide spacer, the addition of TEGDMA causes considerable volumetric shrinkage upon polymerization and enhanced hydrophilicity of the mixture, leading to residual stresses and microcavities, which affect the long-term mechanical characteristics of the composite [11,17,18]. Moreover, bacteria can enter the tooth micro-gaps [19], forming biofilms and releasing acids, which may result in demineralization and tooth decay [20].

To overcome these effects, substantial efforts have been made by researchers to tailor the rheological and structural properties of BisGMA and develop BisGMA analogs with low viscosity and high hydrophobicity, such as hydroxyl-free propoxylated BisGMA (CH_3Bis-GMA) and propoxylated fluorinated BisGMA (CF_3Bis-GMA), as replacements for TEGDMA in BisGMA mixtures [21,22]. Kim et al. [23] replaced the hydroxyl groups in BisGMA with methoxy groups, which dramatically decreased the viscosity of BisGMA from 574 to 3.7 Pa s. Consequently, the amount of TEGDMA included in the resin matrix was minimized. Similarly, Wang et al. [24] synthesized two analogs of BisGMA via an esterification reaction by using benzoyl and valeryl as substituent groups for the hydroxyl groups. Their results showed that the viscosity of BisGMA was dramatically reduced from 820 Pa s to 2.7 and 1.6 Pa s by regulating the size of the benzoyl and valeryl substituent groups, respectively.

The objective of the present study was to fabricate a BisGMA analog via chemical modification, replacing the hydroxyl group with a less hydrophilic substituent group, i.e., chlorine, to synthesize chlorinated BisGMA (Cl-BisGMA). The Cl-BisGMA was synthesized using the Appel reaction in an inert nitrogen atmosphere. Our hypothesis was that the newly synthesized Cl-BisGMA would have a lower viscosity than BisGMA and exhibit promising physical properties for use as an alternative to BisGMA.

2. Materials and methods

2.1. Materials

BisGMA (>98%), TEGDMA (>95%), 2-(N, N-dimethyl amino) ethyl-methacrylate (DMAEMA; 98%), CQ (97%), and carbon tetrachloride (CCl_4; >99.8%) were purchased from Sigma–Aldrich, Germany. Triphenylphosphine (Ph_3P; >98%) was obtained from Cica-reagent (Kanto Chemical, Japan). *n*-Hexane (Hx; >97%) was purchased from Avonchem, UK. Ethyl acetate (EA; 99%) was obtained from Fisher Scientific, UK. All the chemicals were used as received, without further purification.

2.2. Methods

2.2.1. Synthesis of monomer (Cl-BisGMA)

Cl-BisGMA was synthesized via the Appel reaction [25–27] in an inert nitrogen atmosphere. The reaction was conducted in a three-necked flask equipped with a magnetic stirring bar and a reflux condenser. Initially, 26.59 g of Ph_3P (0.1014 mol) was added to a stirred solution of BisGMA (0.0390 mol, 20.00 g) with an excess amount of CCl_4 (0.7249 mol, 70.13 mL). The reaction mixture was stirred under reflux for 2 h, and the progress of the reaction was monitored according to the disappearance of BisGMA via thin-layer chromatography (TLC). Subsequently, the mixture was allowed to cool to room temperature and filtered through a pad silica. Dry hexane (150 mL) was added to the filtrate, and the Ph_3Poxide precipitate was filtered. The solvent was removed using a rotary evaporator, and the Cl-BisGMA was purified through flash column chromatography (FCC) using EA/hexane (7:3 by volume) as an eluent. The fractions from FCC were spots on the TLC aluminum plates, and the Cl-BisGMA-containing fractions were collected accordingly. After the solvent was removed, a clear, light yellow, low-viscosity product was obtained, with a final yield of 13.5 g (63%). This product was kept in a dark container at 8 °C for further experiments. The reaction route for Cl-BisGMA prepared via the Appel reaction is shown in Scheme 1a. The substitution of OH by Cl occurs through a second-order nucleophilic (S_N2) mechanism. The reaction begins with the formation of the phosphonium chloride (3). The deprotonation step of BisGMA (5) yields the alkoxide-form (7) which attacks the phosphonium ion resulting in an intermediate (9) and an active chloride ion (8). Finally, the oxygen is transferred into the leaving group triphenylphosphine oxide (10), and the S_N2

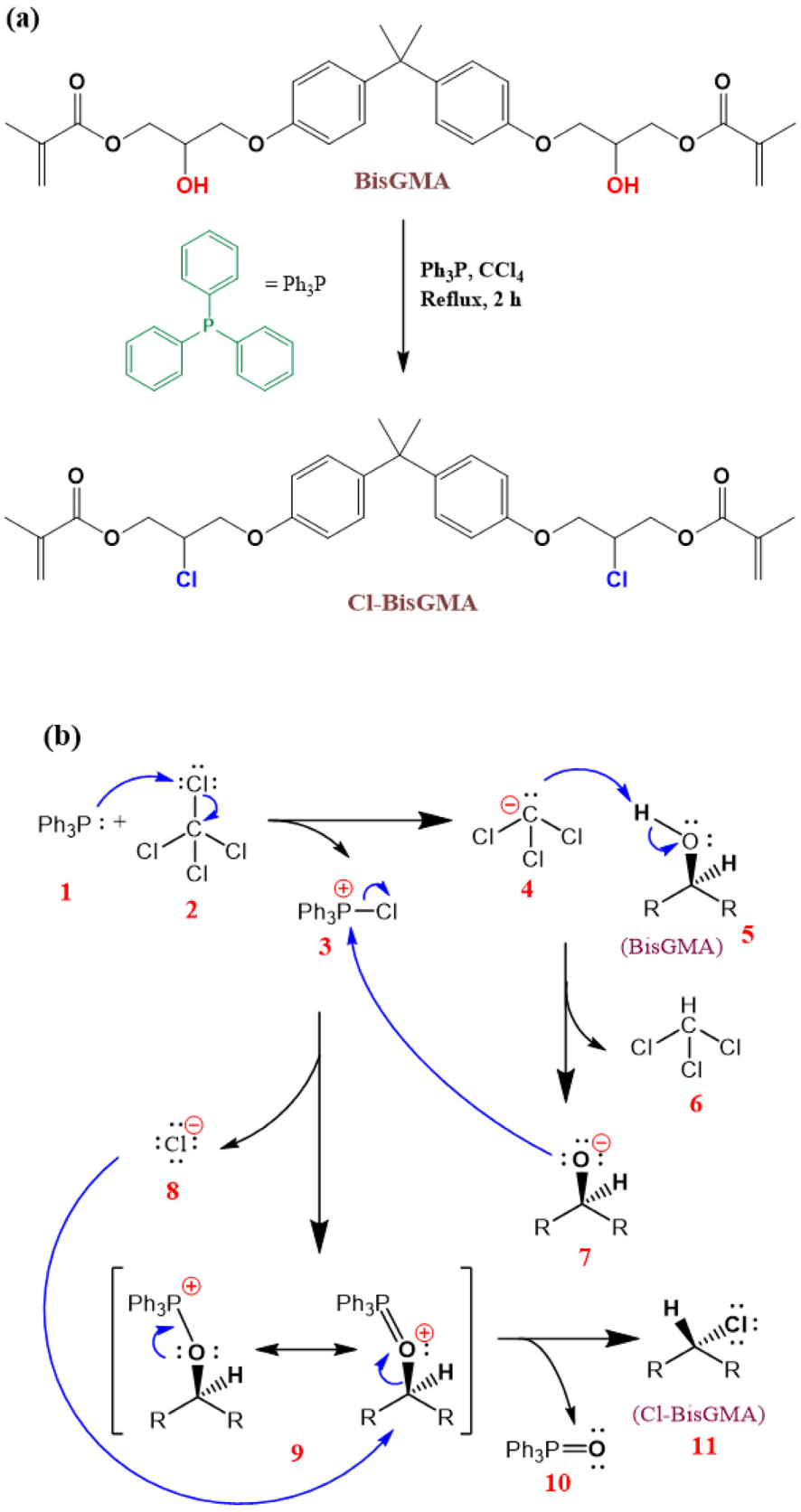

Scheme 1 – Synthesis of the Cl-BisGMA monomer; reaction route (a) and reaction mechanism (b).

displacement by chloride takes place, resulting in Cl-BisGMA (11) with inverted configuration (Scheme 1b).

The chemical structure of Cl-BisGMA was confirmed via Fourier transform infrared (FTIR) spectroscopy, nuclear magnetic resonance (NMR) spectroscopy, and mass spectrometry (MS). The FTIR spectra were recorded using an FTIR spectrometer (Nicolet iS10, Thermo Scientific, USA) with attenuated total reflection (ATR; diamond crystal) accessories. The spectra were obtained in the range of 4000–500 cm^{-1} with a total of 32 scans per spectrum and a resolution of 4 cm^{-1}. The mass spectrum was obtained using an Accu-TOF LC-plus JMS-T100 LP atmospheric pressure ionization ToF-MS spectrometer (JEOL, Tokyo, Japan) equipped with a DART ion source (IonSense, Saugus, USA) and operated in the + ve-ion mode. Selected peaks were assigned using the MassCentre software (version 1.3.m). The NMR spectra were recorded using a DELTA_NMR spectrometer (JEOL Resonance, JEOL, Japan) with a field strength of 400 MHz and eight total scans at 22.1 °C, by employing deuterated chloroform ($CDCl_3$) as the solvent and tetramethylsilane as the internal standard. The data were visualized using the Delta 5.0.4 software, and the chemical shift was presented in parts per million (ppm).

1H and 13C NMR (400 MHz, $CDCl_3$) δ [ppm]: BisGMA = 1H NMR: 7.23 (m, 4H, H-4), 6.91 (m, 4H, H-5), 6.24 (s, 2H, H-12a), 5.68 (s, 2H, H-12b), 4.51-4.20 (m, 6H, H-8 and H-9), 4.20-3.95 (m, 4H, H-7), 3.18 (s, 2H, H-14), 2.04 (s, 6H, H-13), 1.72(s, 6H, H-2); 13C NMR: 167.02 (C-10), 155.85 (C-6), 143.09 (C-3), 135.46 (C-11), 127.29 (C-4), 125.92 (C-12), 113.54 (C-5), 77.00 ($CDCl_3$), 68.38 (C-7), 67.82 (C-8), 65.22 (C-5), 41.19 (C-1), 30.58 (C-2), 17.82 (C-13). Cl-BisGMA = 1H NMR: 7.23 (m, 4H, H-4), 6.90 (m, 4H, H-5), 6.24 (s, 2H, H-12a), 5.68 (s, 2H, H-12b), 4.68-3.82 (m, 10H, H-7, H-8 and H-9), 2.07 (s, 6H, H13), 1.72 (s, 6H, H-2); 13C NMR: 166.38 (C-10), 155.66 (C-6), 143.71 (C-3), 135.50 (C-11), 127.61 (C-4), 126.14 (C-12), 113.89 (C-5), 77.00 ($CDCl_3$), 68.30 (C-7), 64.54 (C-9), 55.18 (C-8), 41.52 (C-1), 30.77 (C-2), 18.02 (C-13).

2.2.2. *Preparation of resin mixture*

The composition and mass ratios of various formulations (F1–F5) are presented in Table 1. The typical preparation procedures for these photocurable resins were as follows.

The photoinitiator system comprising CQ and DMAEMA (0.2 wt.% and 0.8 wt.% based on the total monomer weight, respectively) was mechanically mixed with the appropriate monomers. The mixture was sonicated in an ultrasonic water bath for 2 min and mixed again in a dual asymmetric centrifugal mixing system (Speed Mixer TM DAC 150 FVZ, Hauschild & Co., Hamm, Germany) three times (for 1 min each) at 2500 rpm. After mixing, the obtained resins were deaerated in vacuum for 15 min at room temperature. Each group consisted of two monomers with the ratio 70:30, except for F5, to which 15 wt.% of the monomer TEGDMA was added to equal ratios (wt.%) of BisGMA and Cl-BisGMA owing to the high viscosity of the mixture.

2.2.3. *Rheological measurement of uncured resins*

The viscosity of the resins (F1–F5), in addition to BisGMA and TEGDMA monomers was measured using a rheometer (MCR 72, Anton Paar, USA), with a 25 mm parallel plate geometry and 0.5 mm gap at 22.1 °C (n = 3). The test was performed under steady shear rate ranging from 0.01 to 1000 (1/s).

2.2.4. *Degree of double-bond conversion (DC)*

The DC was determined via ATR-FTIR spectroscopy. A plastic mold (5 mm in diameter and 2 mm thick, n = 5) between a pair of glass slides (0.1 mm thick) was filled with the resin and irradiated for 40 s, using a light-curing unit (3 M ESPE Elipar S10, LED curing light; wavelength of 430–480 nm; intensity of approximately 1200 mW cm^{-2}). The DC was calculated according to the change of the photopolymerizable C=C (vinyl) band area at m^{-1} (A_{1638}) compared with the unaffected aromatic C=C band area of bisphenol A at 1608 cm^{-1} (A_{1608}) before and after light curing using Eq. (1).

$$DC\,(\%) = \left[1 - \frac{\left(\frac{A_{1638}}{A_{1608}}\right) cured}{\left(\frac{A_{1638}}{A_{1608}}\right) uncured}\right] \times 100 \quad (1)$$

2.2.5. *Water sorption and solubility test*

The water sorption and solubility test was carried out by following ISO 4049 [28]. Disc-shaped specimens (15 mm in diameter and 2 mm thick, n = 5) were prepared in a plastic ring mold and light-cured from both sides (for 40 s each) using a curing unit (3M ESPE Elipar S10) with a 10-mm-diameter curing tip in four overlapped areas. The specimens were kept in a desiccator containing dried silica gel and maintained at 37 ± 2 °C for 24 h. They were then transferred into another desiccator, maintained at 23 ± 1 for approximately 1 h, and weighed. The drying process was repeated until a constant weight was obtained, which was measured with an accuracy of 0.1 mg (m1). After final drying, the specimens were immersed in 15 mL of distilled water at 37 ± 2 °C for 24 h. Then, they were removed, carefully swabbed, waved in the air for 30 s, weighed, and returned to the water. The water sorption cycle was repeated until a constant weight was obtained (m2). The specimens were then removed from the water and dried in the desiccator at 37 ± 2 °C until a constant weight was obtained (m3). The values of the water sorption (W_{SP}) and solubility (W_{SL}) were calculated using Eqs. (2) and (3).

$$W_{SP}\,(\%) = \left(\frac{m_2 - m_1}{m_1}\right) \times 100 \quad (2)$$

$$W_{SL}\,(\%) = \left(\frac{m_1 - m_3}{m_1}\right) \times 100 \quad (3)$$

2.2.6. *Cytotoxicity analysis*

Disc-shaped specimens (5 mm in diameter and 2 mm thick, n = 5 for each group) were prepared for cytotoxicity studies. One side of each disc was subjected to an abrasive process using Korox 110 sand and kept under sterilized conditions until use. Immortalized human bone marrow stromal cells (TERT-hBMSCs) produced by the forced overexpression of the human telomerase reverse transcriptase gene in primary hBMSCs [29,30] were used. A subclone derived from TERT-hBMSCs described as CL1, which exhibits an enhanced osteogenic, adipogenic, and chondrogenic differentiation potential, was cultured as previously described [31].

Table 1 – Compositions of the resins with the experimental formulations.

Formulation	BisGMA wt.%	TEGDMA wt.%	Cl-BisGMA wt.%	Initiator system (wt.%, with respect to the total monomers)	
				CQ wt.%	DMAEMA wt.%
F1	70	30	0	0.2	0.8
F2	0	30	70	0.2	0.8
F3	0	0	100	0.2	0.8
F4	30	0	70	0.2	0.8
F5	42.5	15	42.5	0.2	0.8

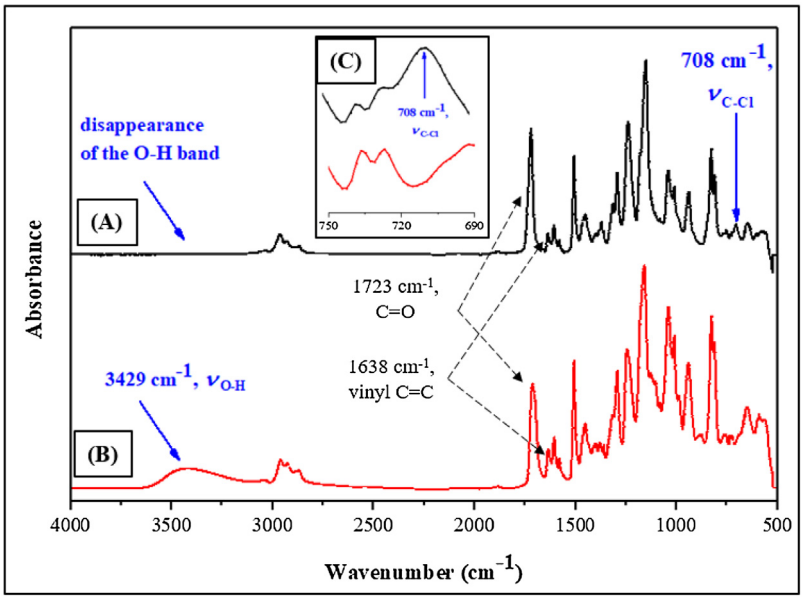

Fig. 1 – FTIR spectra of (A) Cl-BisGMA and (B) BisGMA. The inset (C) shows a magnified view of the C-Cl region.

2.2.6.1. Stromal-cell attachment and morphology assessment. Three days after the CL1 stromal cells were added to the various prepared resin discs, the cell attachment was observed using scanning electron microscopy (SEM). For this, CL1 cells were added to five different discs. The discs were soaked overnight in fetal calf serum to improve the cell attachment. On the day of cell seeding, the discs were washed once with the growth media, and then 1×10^5 cells were added to each disc. On day 3, each disc was washed with a phosphate-buffered solution and fixed with 1% glutaraldehyde (Sigma–Aldrich, St. Louis, MO, USA) buffered in 0.1 M sodium cacodylate (Agar Scientific, Stansted, UK) at 4–6 °C for SEM sample preparation. After glutaraldehyde fixation, the cells were fixed in 1% osmium tetroxide (Agar Scientific, Stansted, UK) according to the instructions from the manufacturer. The dry specimens were sputter-coated with gold and examined using a Carl Zeiss Sigma VP Oxford Micro-analysis S800, as previously reported [32]. The discs were subsequently observed, and images were captured using a JSM-6360 LV scanning electron microscope.

2.2.6.2. Cell viability assay using alamarBlue®. The cell viability of the CL1 cells grown on the resin discs was assessed via an alamarBlue® cell viability assay performed according to recommendations from the manufacturer (AbD Serotec, Raleigh, NC, USA). Briefly, 10 µL of the alamarBlue® substrate was added directly to the cultured cells. The cells were cultured in a 96-well plate after the addition of alamarBlue® and incubated at 37 °C for 1 h in darkness. The fluorescence was measured using an Ex530 nm/Em 590 nm with a BioTek Synergy II plate reader (BioTek Inc., Winooski, VT, USA).

2.2.6.3. Live/dead assay. CL1 cells were plated onto the five prepared discs at a density of 1×10^4 cells/mL in 2 mL of culture medium. The plate was incubated at 37 °C under 5% CO_2 for three durations: 4, 10, and 14 d. A live/dead stain was prepared by adding 2 µmol/L acetomethoxy derivate of calcein (calcein-AM) and 2 µmol/L ethidium homodimer-1 per milliliter of medium. The construct was then left in the incubator for 30 min; subsequently, the dye was removed and replaced with 1 mL of DMEM. Observation was performed on the same day using fluorescent microscopy (Leica-Letiz DM IRB, Wetzlar, Germany). Three random fields of view were chosen at a low objective magnification (5×), and then five areas were observed at 10× using an Axiovision camera (Zeiss, Jena, Germany; a total of three constructs yielded 15 images for each cement). The mean live and mean dead cell numbers were estimated according to the five images. Then, the percentage of viable cells was determined by dividing the mean number of live cells by the total cell count (live and dead cells).

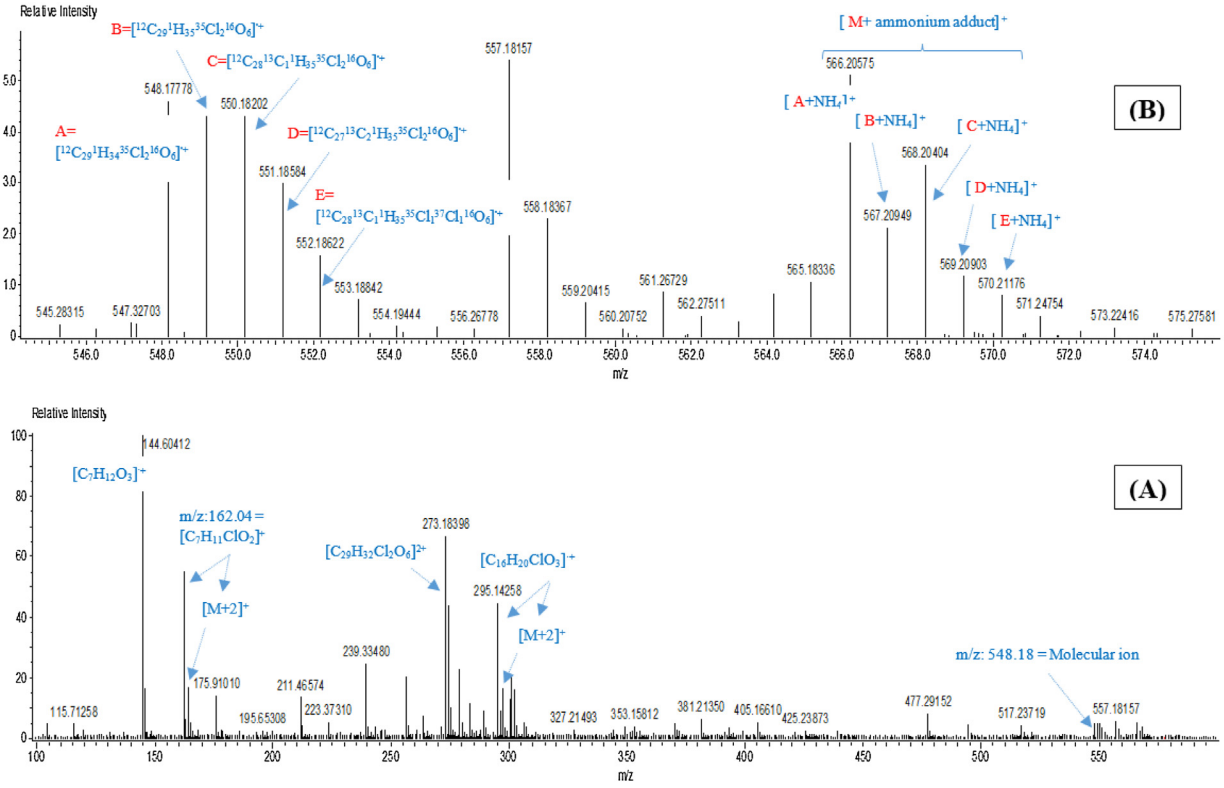

Fig. 2 – DART mass spectra of Cl-BisGMA: (A) full fragmentation pattern and (B) molecular-ion region magnification.

2.2.7. *Statistical analysis*

One-way analysis of variance and Tukey post-hoc tests (SigmaPlot 12.5, Systat Software Inc., London, UK) were used to analyze the significance of the viscosity, DC, water sorption, and solubility. All data were subjected to Levene's test of homogeneity of variance ($\alpha = 0.05$), following the assumption of equal variances.

3. Results

3.1. *FTIR spectroscopy*

The substitution of chlorine for the hydroxyl groups of BisGMA was confirmed via FTIR spectroscopy. Fig. 1 shows the FTIR spectra of Cl-BisGMA and BisGMA. In the spectra of BisGMA (Fig. 1B), the broad band at 3429 cm^{-1} is attributed to the hydroxyl (OH) groups of BisGMA. The disappearance of the OH band in the spectrum of Cl-BisGMA (Fig. 1A) confirms its replacement by chlorine atoms [33]. Moreover, the band corresponding to the C-Cl bond in Cl-BisGMA (Fig. 1C) is observed around 708 cm^{-1} [34], confirming the replacement of the OH group. Additionally, the FTIR spectra exhibit peaks at 1723 and 1638 cm^{-1}, indicating the presence of carbonyl and vinyl groups, respectively, in both BisGMA and Cl-BisGMA.

3.2. *Mass spectrometry*

The profile of the Cl-BisGMA mass fragments obtained using the high-resolution DART-ToF-MS spectrometer is shown in Fig. 2A. The observed peaks for the m/z fragments were assigned and confirmed through the calculated fragmentation pathway of the molecule. The peaks at m/z = 144.60 and 548.18 are the base peak and the peak corresponding to molecular ion, respectively. Chlorine is an important atom in MS because its fragmentation reflects its two most stable, naturally abundant isotopes—^{35}Cl (75.78%) and ^{37}Cl (24.22%) [35]—with MS peaks separated by m/z = 2 and a relative intensity of 3:1 for an ion with a single chlorine atom and 9:6:1 for an ion with two chlorine atoms [34]. Fig. 2B shows the parent ion (molecular ion) $[M]^+$ and its ammoniated adduct $[M + NH_4]^+$ at m/z = 548.18 and 566.20, corresponding to peak-(A) and peak-(A + NH_4), respectively [36]. The overall profile of the peaks (A to E) and their ammonium adducts are identical, and their intensities indicate the existence of two chlorine atoms in the molecule (peak intensity ratio of 9:6:1 for $[M]^+$:$[M+2]^+$:$[M+4]^+$), which is more clear for the ammoniated ion peaks. Lower mass fragments with one chlorine atom are also observed, and their m/z values are assigned as shown in Fig. 2A. For example, the peaks at m/z = 162.04 and 164.04 agree with the typical intensity ratio of a single chlorine atom-containing molecule with an intensity ratio of 3:1 for $[M]^+$:$[M+2]^+$. Similar patterns are observed for all the chlorine-containing fragments.

3.3. *Nuclear magnetic resonance spectroscopy*

The chemical structure of Cl-BisGMA was confirmed via ^1H and ^{13}C NMR spectroscopy, as shown in Figs. 3 and 4, respectively. The spectra of Cl-BisGMA were exactly the same as those of BisGMA, except for peaks 7, 8, and 9, which correspond to the substitution center (peak-8) and the adjacent

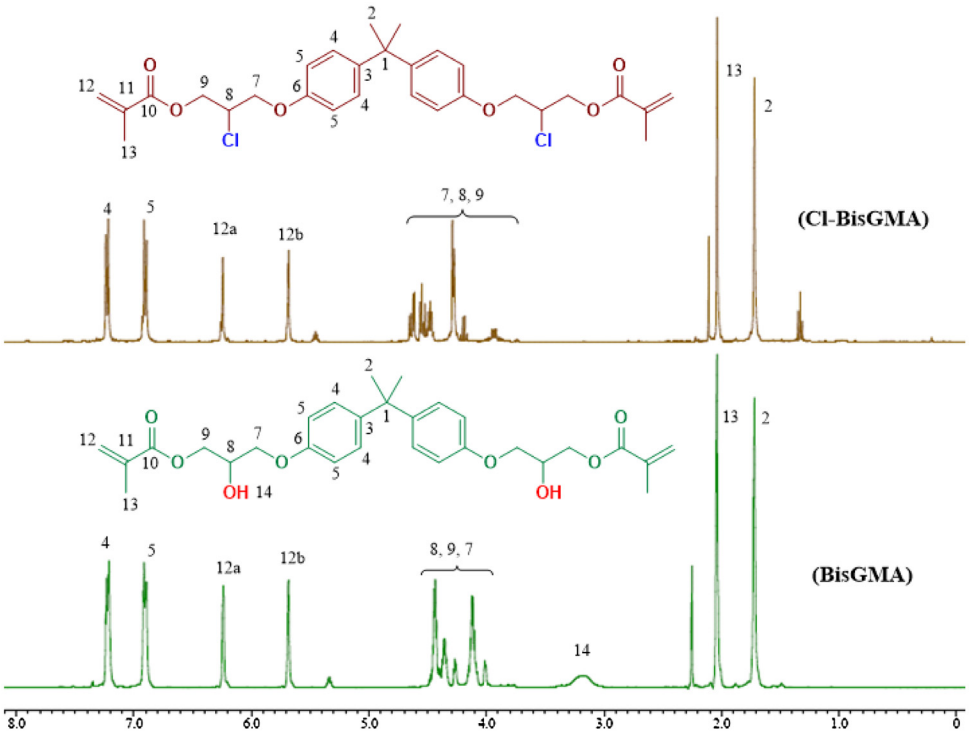

Fig. 3 – ^{1}H NMR spectra of BisGMA and Cl-BisGMA in $CDCl_3$.

positions (peaks 7 and 9). The BisGMA ^{1}H and ^{13}C NMR spectra are similar to those previously reported [24,33,37]. For ^{1}H NMR, the chemical shift of the OH proton is variable owing to the H-bonding and proton exchange, and its position (0.5–5.0 ppm) depends on the concentration, solvent, temperature, etc. [34]. In the literature [24,33,38], the BisGMA OH peak for $CDCl_3$ is reported as a broad single peak between 2.2 and 2.6 ppm. In Fig. 3, the singlet peak at 3.18 (H-14) ppm in the BisGMA spectrum is attributed to this OH proton. However, the Cl-BisGMA spectrum shows no similar peak in this region, confirming the substitution reaction with chlorine atoms. Additionally, the effect of the OH replacement by chlorine on the adjacent protons is insignificant, as both OH and Cl exhibit closely deshielding behavior [34]. Peaks corresponding to the protons

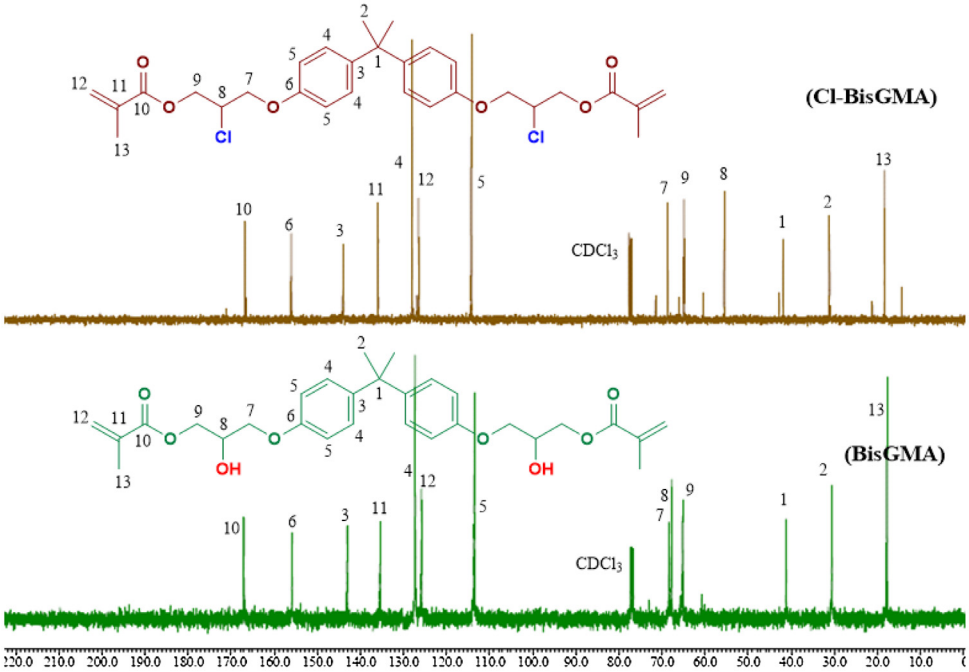

Fig. 4 – ^{13}C NMR spectra of BisGMA and Cl-BisGMA in $CDCl_3$.

Table 2 – Viscosity, DC, water sorption, and water solubility of the different formulations.

Formulation	Viscosity (Pa s)		DC %		W_{SP} (wt.%)		W_{SL} (wt.%)	
	Average	SD	Average	SD	Average	SD	Average	SD
F1	2.26	0.064[a]	62.0	0.63[a]	2.950	0.091[a]	0.301	0.162[a]
F2	0.38	0.035[a]	70.6	0.80[b]	0.408	0.061[b]	0.350	0.036[a]
F3	7.22	1.105[b]	60.4	0.21[a]	0.115	0.119[c]	0.650	0.257[b]
F4	41.15	1.349[c]	50.1	2.15[c]	0.250	0.074[c,b]	0.657	0.085[b]
F5	5.56	1.305[b]	56.8	2.00[d]	1.093	0.176[d]	0.337	0.008[a]

The same superscript indicates no significant difference ($p < 0.05$).

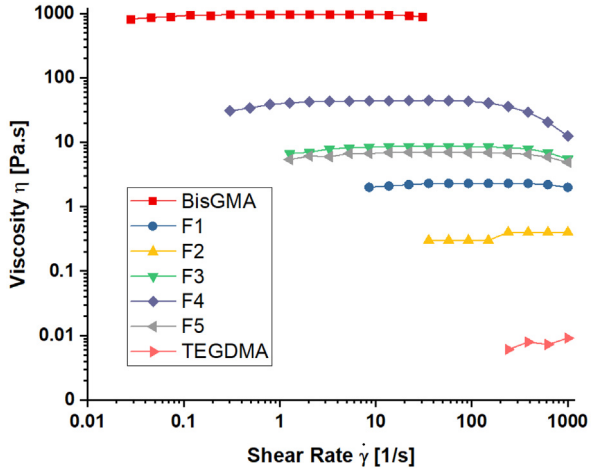

Fig. 5 – Viscosity measurement of BisGMA, TEGDMA and resin systems (F1–F5) at 22.1 °.

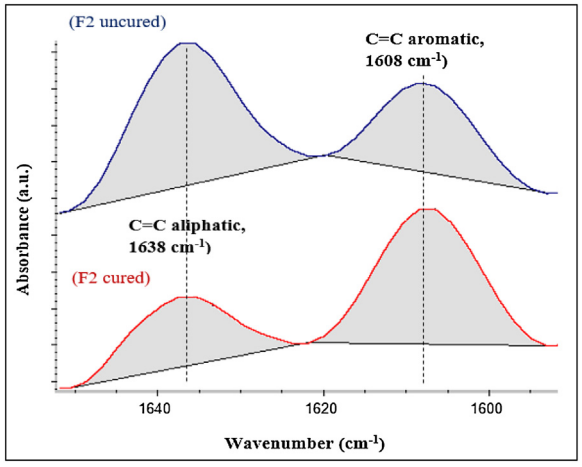

Fig. 6 – Representation of the double-bond conversion for the F2 resin.

in the substitution region (H-7, H-8, and H-9) were observed at 4.5–3.9 and 4.7–3.8 of BisGMA and Cl-BisGMA, respectively. Moreover, the integration of this region for both monomers indicates the presence of 10 protons in total, confirming the proposed chemical structure of Cl-BisGMA. In the ^{13}C NMR spectra, the chemical shifts corresponding to C-7, C-8, and C-9 (Fig. 4) were from 68.38, 67.82, and 65.22 for BisGMA to 68.30, 55.18, and 64.54 ppm for Cl-BisGMA, respectively. The major change was for C-8, which was the center of the substitution reaction (from 67.82 to 55.18 ppm). All the other carbons were unaffected, and similar chemical shifts were observed for both monomers.

3.4. *Viscosity test*

Fig. 5 shows the viscosity of neat BisGMA and TEGDMA in addition to all the other resin systems (F1 to F5), as a function of the shear rate in the range of 0.01–1000 (1/s). All the specimens exhibited a Newtonian behavior with respect to shear rate. The calculated viscosities of BisGMA and TEGDMA monomers were 909.9 and 0.007 (Pa s) respectively, while the resin systems (F1-F5) exhibited viscosities ranged between BisGMA and TEGDMA as given in Table 2. The measured viscosity was ordered as BisGMA > F4 > F3 > F5 > F1 > F2 > TEGDMA.

Among the resin systems (F1 to F5), F4 resulted in highest viscosity while the lowest viscosity was exhibited by F2. F3 and F5 resulted in moderate viscosities however, F1 resulted in lower viscosity than F3 and F5.

3.5. *DC, water sorption, and solubility*

The DC was assessed via FTIR analysis. A representative FTIR spectrum for peak area calculation is shown in Fig. 6. The DC was calculated using Eq. (1) by comparing the changes in the area of the aliphatic C=C peak (vinyl bond) at 1638 cm^{-1} and that of the internal standard peak of aromatic C=C at 1608 cm^{-1} during polymerization, compared with the uncured material.

The mean DC, W_{SP}, and W_{SL} for each test group are presented in Table 2. According to the literature, no significant change in the DC occurs after 40 s of irradiation [39]. Therefore, for all the test samples, the irradiation was conducted for 40 s. The results revealed that F2 exhibited the highest DC (70%) among all the groups, while F4 exhibited the lowest DC (50.1%). F1 and F3 did not show a significant difference in their DC values ($p > 0.05$). However, F5 exhibited a significantly higher DC value than F4 ($p < 0.05$).

F3 showed the lowest water-sorption value (F3 < F4 < F2 < F5 < F1). As expected, F1 (with a BisGMA-to-TEGDMA ratio of 70:30), exhibited the highest water-sorption value. F5, which consisted of an equal proportion of BisGMA and Cl-BisGMA (42.5 wt.% each) and 15 wt.% of TEGDMA, exhibited the second-highest water sorption. F3 (containing 100% Cl-BisGMA) and F4 (70% Cl-BisGMA) did not show any significant difference in water-sorption values ($p > 0.05$). Similarly, F2 (70% Cl-BisGMA) exhibited a W_{SP} value statistically equal to that of F4 ($p > 0.05$). For F2 and F4, the concentration

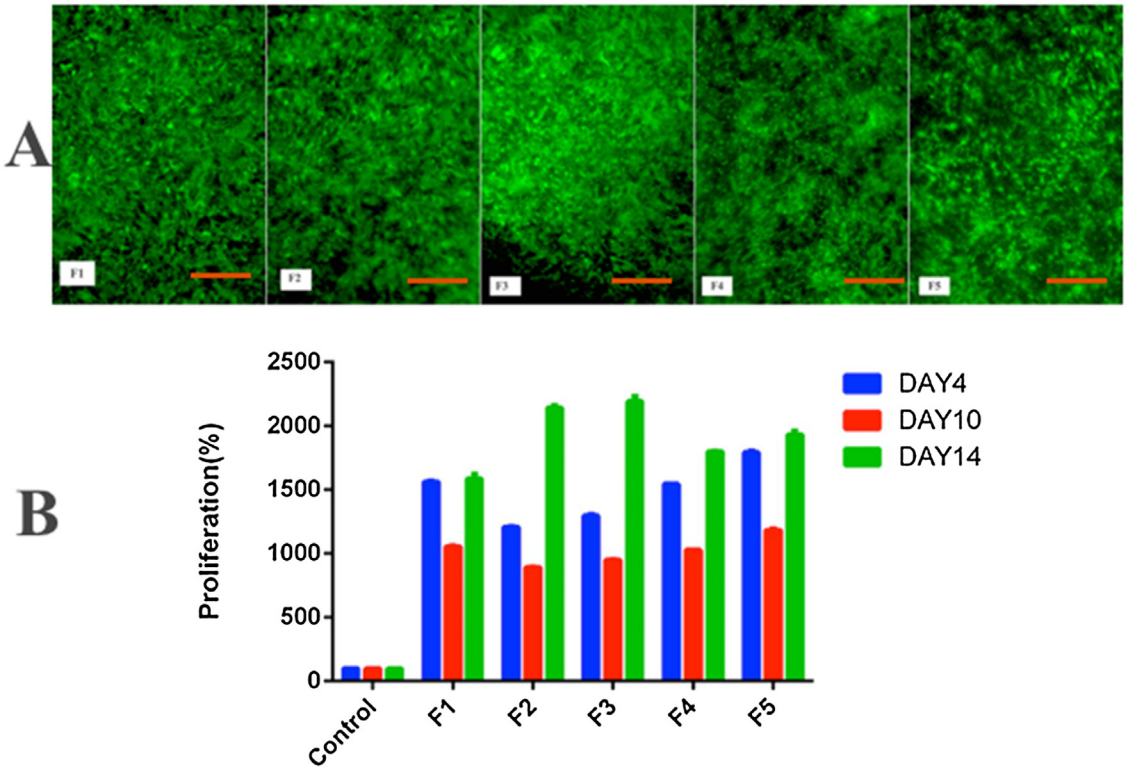

Fig. 7 – (A) CL1 cells grown on resin discs F1–F5 and stained with ethidium homodimer and calcein, which turns all nucleated cells green. The magnification used was 10 × (scale bar =200 μm). (B) AlamarBlue® assay of CL1 cells cultured on the same resin discs. The data show a high CL1 metabolism for F2 and F3 after 14 d of cell culturing. (For interpretation of the references to color in this figure legend, the reader is referred to the web version of this article.)

of Cl-BisGMA was 70 wt.%, in combination with 30 wt.% of TEGDMA and BisGMA, respectively. TEGDMA have adverse effects on properties such as water uptake and curing shrinkage [23]. Thus, the main factor influencing the W_{SP} was the percentage of TEGDMA (30%) in F2 and BisGMA (30%) in F4, as indicated by the W_{SP} values of F1 and F5. F1 contained 70 wt.% of BisGMA and exhibited the highest W_{SP} value, followed by F5, which had the second-highest percentage of BisGMA. On the other hand, F3 (Cl-BisGMA) exhibited significantly reduced W_{SP} values.

Interestingly, the water-solubility order differed from that of the water sorption, with F1, F2, and F5 showing no statistically significant differences in the W_{SL} values. F3 and F4 also exhibited similar W_{SL} values, which were higher than those of the other three compositions. The high values of W_{SL} for F3 and F4 could be related to the presence of unreacted monomer and the low DC due to the absence of low-viscosity TEGDMA in these groups.

4. Biological study

4.1. *Morphological observation of stromal-cell attachment*

SEM images of CL1 proliferating on the surface of each sample disc, covering the surface in the form of layers, are shown in Fig. 7. After 3 d of culturing (CL1) cells, for all five discs, most of the cultured cells adhered to and were clearly observable on the disc surface, with no significant difference between the examined samples, as shown in Fig. 7. However, the cells proliferated to greater extent in some areas, forming cell aggregates. Their shapes were either polygonal or fusiform, accompanied by filamentous fibers formed on the surface, indicating extracellular matrix formation. Furthermore, cells were observed in the pore area and intermingled within the resin material (see Fig. 8C–F). At the periphery of the discs, few cells were detected (Fig. 9). Although the cells reached the desired size and shape, they were unevenly distributed throughout the examined surfaces. This may indicate that the chemical composition of the specimens neither affected the cell survival nor expressed a transgene, as demonstrated by Bianchi et al. [40]. The tested specimens provided a suitable micro-environment for the CL1 cells, supporting their attachment, adhesion, and proliferation. Moreover, the material guided the fate of the seeded cells by selecting subpopulations and influencing their fate, as studied by Bianchi et al. [40]. Our observations suggest that CL1 cells found their niche, interacting with various other cells via cell adhesion. The extracellular matrix is deposited by the niche cells under the influence of integrin receptors and other signaling molecules, including autocrine, paracrine, and endocrine factors. Additional variables include the O_2 tension, pH, ionic load, and glucose strength [40]. These factors can explain the

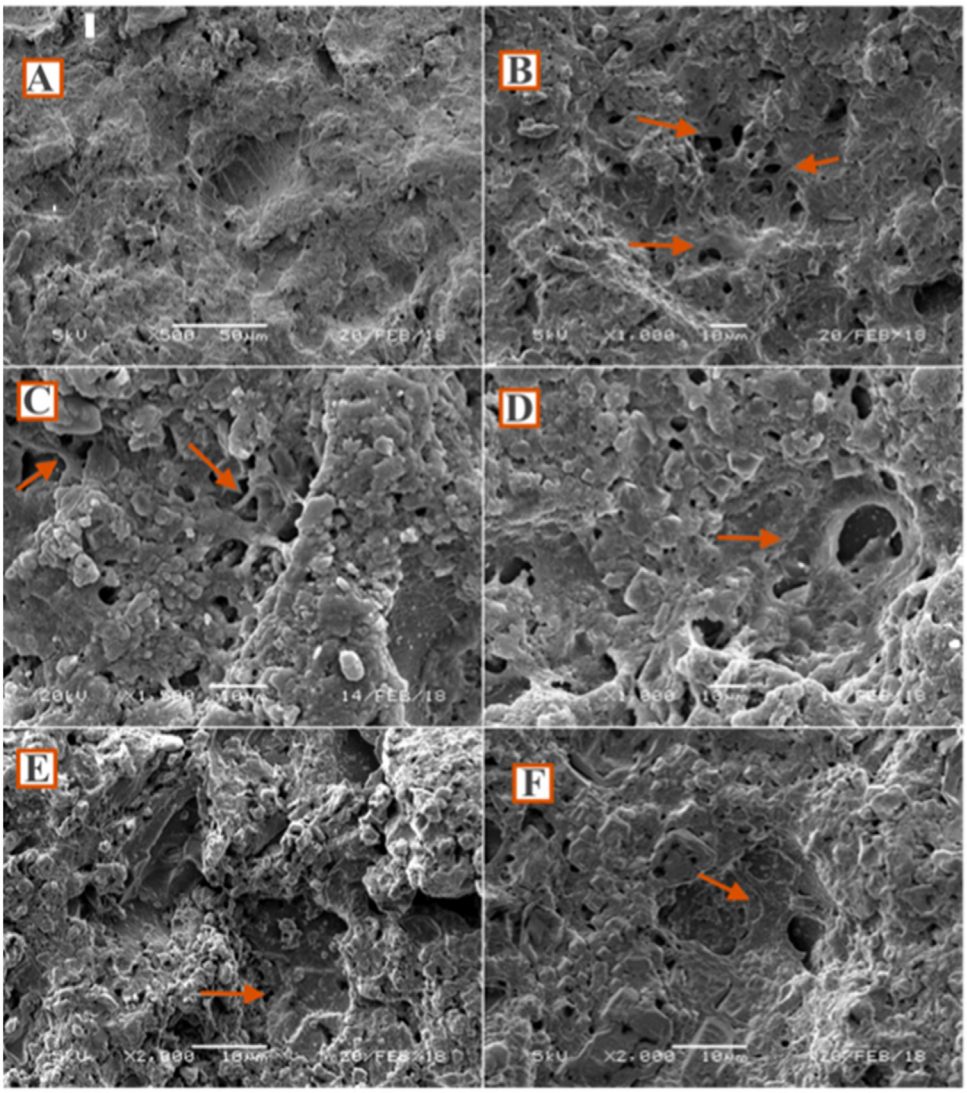

Fig. 8 – SEM images of (A) CL1 proliferating on the surface of the resin disc, covering the surface in the form of layers, and (B) cells spreading on the surface of the resin in layers, as indicated by the red arrows. (C–F) With further magnification, cells were observed in the pore areas, as indicated by the red arrows, exhibiting a normal size (60–160 μm) and shape (polygonal and fusiform) on the surface of the resin discs after 3 d of culturing. The scale bar represents 50 μm in (A) and 10 μm in (B)–(F). (For interpretation of the references to colour in this figure legend, the reader is referred to the web version of this article.).

uneven distribution of cells between the center and periphery of the examined discs.

4.2. *AlamarBlue® assay and live/dead stain*

The percentage of viable cells on the surface of the five discs varied among days 4, 10, and 14. The cell growth exhibited a homogenous trend at different times. A high cell metabolism was observed on day 4, with no statistically significant difference between the specimens. On day 10, a decrease in cell metabolism was observed, which could have been due to cellular senescence. Surprisingly, the cell proliferation indicated an increased metabolism on day 14. The highest reading was reported for F2 and F3, whose values showed a statistically significant difference from those of the other examined discs ($p < 0.05$). The percentage of viable CL1 cells on the disc surface was easily calculated for the five discs after the first 4 d of culturing: 90.6% ± 12%, 77.0% ± 7%, 69% ± 13, 88.5 ± 5%, and 92% ± 15 for F1, F2, F3, F4, and F5, respectively. In general, more cells were observed at the center of the discs than at the borders.

5. Discussion

BisGMA is a high-viscosity monomer owing to the secondary hydroxyl groups and aromatic rings π–π interactions. The high viscosity and strong intermolecular interaction result in a low DC and cause hydrophilicity. In this study, we synthesized a chemically modified BisGMA analog by replacing the OH group of BisGMA with chlorine in order to reduce

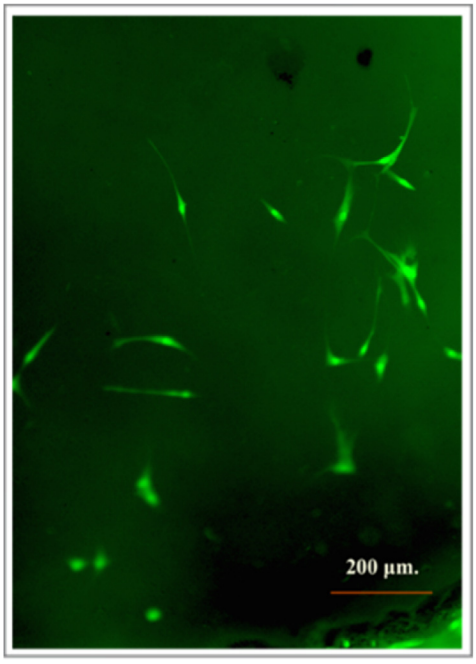

Fig. 9 – Live/dead assay of CLI cells. The image was taken from the borders of the discs, and few cells were detected (scale bar represents 200 µm).

the viscosity. All the tested specimens including BisGMA and TEGDMA exhibited a Newtonian behavior. The neat BisGMA and TEGDMA exhibited the highest and the lowest viscosities (909.92 and 0.007 Pa s, respectively) among all the groups which are in agreement with literatures [41]. The high viscosity of BisGMA is attributed to the strong intermolecular H-bonds caused by hydroxyl groups. This also may be the source of the shear rate dependence of the viscosity observed in F4. At high shear rate (e.g. > 100 1/s), F4 exhibited a gradual shear thinning behavior as a result of H-bonds disruption caused by the high shear forces, however such behavior was also reported for BisGMA and high BisGMA-content resins [39]. F3 (Cl-BisGMA) resulted in significantly lower viscosity (7.22 Pa s) than that of BisGMA (909.92 Pa s), reflecting the disappearance of network junctions, such as hydrogen bonding between monomer molecules, caused by the replacement of the hydroxyl group with chlorine. In comparison, F4 exhibited a higher viscosity (41.15 Pa s), possibly owing to the presence of high molecular weight BisGMA (30 wt.%; MW = 512.6) and absence of TEGDMA.TEGDMA is used as a diluent, as it disrupts hydrogen bonding and acts as an internal lubricant. However, the addition of TEGDMA leads to considerable polymerization shrinkage and high hydrophilicity [39]. The low viscosities of F1 (2.26 Pa s) and F2 (0.38 Pa s) could be attributed to the presence of 30 wt.% of TEGDMA in these resin systems, which has a low MW and very low viscosity. The same effect is reflected in F5 (5.56 Pa/s) which contains a portion of 15 wt.% TEGDMA. The viscosity value of F1 (2.26 Pa s) obtained in this study is in agreement with the literature [41,42].

F2 exhibited the highest DC and the lowest viscosity among the other groups, which is attributed to the presence of TEGDMA in combination with Cl-BisGMA and the absence of strong intermolecular hydrogen bonding, which restrict the molecular movement of the resin. In comparison to F2, F1 exhibited a lower DC value with the same proportion of TEGDMA due to the strong intermolecular interaction caused by H-bonding in BisGMA.

The water sorption of dental composites is related to the physical–chemical properties of their components; the nature of the formed network, such as the three-dimensional structure of the obtained polymer network, the DC, and the free volume entrapped within the structure [43]; and the hydrophilicity and solubility of the network [44,45].

Generally, the water sorption increases with the decrease of the DC [44]. In this study, as expected, F3 exhibited the lowest water sorption, followed by F4, F2 and F5, owing to the relatively low hydrophilicity of Cl-BisGMA. The conventional monomer composition (F1) exhibited the highest water sorption, which is attributed to the high proportion of hydrophilic BisGMA in combination with TEGDMA. It is evident from the literature that both TEGDMA and BisGMA are highly hydrophilic monomers [46,47]. This is confirmed by the present water-sorption results. F5 exhibited the second-highest water sorption, which is attributed to the presence of hydrophilic BisGMA and TEGDMA.

Water solubility is another very important parameter for dental materials. In our study, F3 and F4, despite exhibiting low W_{SP} values, showed the highest solubility. The high water solubility of F3 and F4 may be due to the presence of unreacted monomer after irradiation and low DC. The high W_{SL} for these groups could be attributed to their low DC values. The low DC could be attributed to high viscosities of these groups having no TEGDMA. On the other hand, F1, F2, and F5 showed no significant difference in their W_{SL} values ($p > 0.05$), which could be attributed to their higher DC due to presence of TEGDMA in these groups. Moreover, in case of F1 and F5, the high degree of crosslinking and molecular interaction in the presence of the OH groups in BisGMA could also be related to their low W_{SL}. However, F2 (having 30 wt.% of TEGDMA) resulted in highest DC (70%), leaving minimum un-leached monomer after irradiation, could also be associated to its lower W_{SL}. The solubility of resin composites is related to the dissolution and leaching of various components, particularly unreacted monomers [48]. The density of the links in methacrylate-based resin composites may vary as a result of the polymerization of free radicals, causing spatial heterogeneity that may facilitate the entrapment of residual monomers in microgels, from where they may be easily leached [49]. The addition of TEGDMA in these three groups (F1, F2, and F5) facilitated the polymerization process owing to its very low viscosity and linear structure. This resulted in a reduced quantity of the unreacted monomer and un-leached components. Thus, there was a significant difference in the water-solubility performance compared with the other two groups (F3 and F4). The results indicated that the W_{SP} and W_{SL} values generally change in the same way [50]. In previous studies [46,48,51], materials with low sorption exhibited low solubility. However, researchers have suggested that materials with high water sorption do not necessarily have high solubility [52], as observed in our study.

Assessments of the cell morphology using SEM and cell proliferation and cytotoxicity tests indicated that all the used resin discs were biocompatible during CL1 incubation. How-

ever, a decrease of the cell metabolism was observed on day 10 for all the tested samples. This could be because some of the cells reached cellular senescence, especially at the center of the discs; then, the cells at the borders of the discs proliferated more quickly toward the center. This was observed during live/dead microscopic examination, as shown in Fig. 7. Few cells were observed on day 4 of the culturing in converse to the center of the discs (Fig. 9). Another reason for the decrease of cell proliferation on day 10 may be that the toxicity of the unreacted resin particles caused a local fluctuation in the pH or ionic strength. F2 and F3 exhibited greater proliferation (statistically significant difference) than the other tested samples.

Qualitatively, CL1 viability assessments involving direct cell seeding onto the resin discs and SEM and cytoskeleton evaluation showed that a large number of cells were adherent and proliferating. Additionally, the typical morphological features of the marrow stromal cells on the surfaces of all the discs were observed. Similar SEM findings were obtained when MG-63 was seeded on a surface of polymethyl methacrylate for use as a bone cement [53]. The literature supports the use of in vitro cell cultures as a reliable and sensitive approach to evaluate the biocompatibility of bio-scaffolds [53,54]. In contrast, Bhanushali et al. suggested that although in vitro cytotoxicity tests appear to be sensitive, they cannot replace animal experimentation [55]. Our future challenge is to test the F2 and F3 dental resin composites using a suitable model in vivo.

6. Conclusion

Although BisGMA is a common base for dental resin composites, its high viscosity is a major drawback preventing the addition of the desired high filler content. Halogenated derivatives produced via replacement of the OH group are potential solutions, as OH is the major cause of the increased viscosity due to hydrogen bonding. In this study, we successfully synthesized a Cl-BisGMA monomer by replacing the hydroxyl groups (OH) in BisGMA with chlorine atoms. Its low viscosity is worthy of further comprehensive investigation. The tested essential properties, such as the rheology, cytotoxicity, biocompatibility, DC, water sorption, and solubility, were promising, with values similar to or even better than those for BisGMA. The results indicate that Cl-BisGMA can be used as an analog of BisGMA, offering a new approach in the development of dental resin composites with novel properties.

Acknowledgements

The authors are grateful to the Deanship of Scientific Research, King Saud University, for funding through the Vice Deanship of Scientific Research Chairs, Engineer Abdullah Bugshan research chair for Dental and Oral Rehabilitation.

REFERENCES

[1] Conrad HJ, Seong WJ, Pesun IJ. Current ceramic materials and systems with clinical recommendations: a systematic review. J Prosthet Dent 2007;98:389–404.

[2] Cramer N, Stansbury J, Bowman C. Recent advances and developments in composite dental restorative materials. J Dent Res 2011;90:402–16.

[3] Ragain Jr JC, Johnston WM. Color acceptance of direct dental restorative materials by human observers. Color Research & Application: Endorsed by Inter-Society Color Council, The Colour Group (Great Britain), Canadian Society for Color, Color Science Association of Japan, Dutch Society for the Study of Color, The Swedish Colour Centre Foundation, Colour Society of Australia. Centre Français de la Couleur 2000;25:278–85.

[4] De Munck J, Van Landuyt K, Peumans M, Poitevin A, Lambrechts P, Braem M, et al. A critical review of the durability of adhesion to tooth tissue: methods and results. J Dent Res 2005;84:118–32.

[5] Brunthaler A, König F, Lucas T, Sperr W, Schedle A. Longevity of direct resin composite restorations in posterior teeth: a review. Clin Oral Investig 2003;7:63–70.

[6] Ferracane JL. Resin composite—state of the art. Dent Mater 2011;27:29–38.

[7] Ferracane JL. Resin-based composite performance: are there some things we can't predict? Dent Mater 2013;29:51–8.

[8] Stansbury JW. Dimethacrylate network formation and polymer property evolution as determined by the selection of monomers and curing conditions. Dent Mater 2012;28:13–22.

[9] Tamareselvy K, Rueggeberg F. Synthesis and characterization of a monofunctional analog to BIS-GMA: a dental monomer. J Appl Polym Sci 1995;57:705–16.

[10] Truffier-Boutry D, Demoustier-Champagne S, Devaux J, Biebuyck J-J, Mestdagh M, Larbanois P, et al. A physico-chemical explanation of the post-polymerization shrinkage in dental resins. Dent Mater 2006;22:405–12.

[11] Amirouche-Korichi A, Mouzali M, Watts DC. Shrinkage strain – rates study of dental composites based on (BisGMA/TEGDMA) monomers. Arab J Chem 2017;10: S190–5.

[12] Stansbury JW. Curing dental resins and composites by photopolymerization. J Esthet Dent 2000;12:300–8.

[13] Jakubiak J, Allonas X, Fouassier JP, Sionkowska A, Andrzejewska E, Linden LÅ, et al. Camphorquinone–amines photoinitating systems for the initiation of free radical polymerization. Polymer 2003;44:5219–26.

[14] Peutzfeldt A. Resin composites in dentistry: the monomer systems. Eur J Oral Sci 1997;105:97–116.

[15] Lempel E, Czibulya Z, Kovács B, Szalma J, Tóth Á, Kunsági-Máté S, et al. Degree of conversion and BisGMA, TEGDMA, UDMA elution from flowable bulk fill composites. Int J Mol Sci 2016;17:732.

[16] Baroudi K, Mahmoud S. Improving composite resin performance through decreasing its viscosity by different methods. Open Dent J 2015;9:235–42.

[17] Dewaele M, Truffier-Boutry D, Devaux J, Leloup G. Volume contraction in photocured dental resins: the shrinkage-conversion relationship revisited. Dent Mater 2006;22:359–65.

[18] Alvarez-Gayosso C, Barcelo-Santana F, Guerrero-Ibarra J, Saez-Espinola G, Canseco-Martinez MA. Calculation of contraction rates due to shrinkage in light-cured composites. Dent Mater 2004;20:228–35.

[19] Truffier-Boutry D, Demoustier-Champagne S, Devaux J, Biebuyck JJ, Mestdagh M, Larbanois P, et al. A physico-chemical explanation of the post-polymerization shrinkage in dental resins. Dent Mater 2006;22:405–12.

[20] Hicks J, Garcia-Godoy F, Flaitz C. Biological factors in dental caries enamel structure and the caries process in the dynamic process of demineralization and remineralization (part 2). J Clin Pediatr Dent 2004;28:119–24.

[21] Pereira SG, Nunes TG, Kalachandra S. Low viscosity dimethacrylate comonomer compositions [Bis-GMA and CH3Bis-GMA] for novel dental composites; analysis of the network by stray-field MRI, solid-state NMR and DSC & FTIR. Biomaterials 2002;23:3799–806.
[22] Prakki A, Cilli R, Vieira IM, Dudumas K, Pereira JC. Water sorption of CH(3)- and CF(3)-Bis-GMA based resins with additives. J Appl Oral Sci 2012;20:472–7.
[23] Kim JW, Kim LU, Kim CK, Cho BH, Kim OY. Characteristics of novel dental composites containing 2,2-Bis[4-(2-methoxy-3-methacryloyloxy propoxy) phenyl] propane as a Base Resin. Biomacromolecules 2006;7:154–60.
[24] Wang R, Zhu M, Bao S, Liu F, Jiang X, Zhu M. Synthesis of two bis-GMA derivates with different size substituents as potential monomer to reduce the polymerization shrinkage of dental restorative composites. J Mater Sci Res 2013;2:12.
[25] Appel R. Tertiary phosphane/tetrachloromethane, a versatile reagent for chlorination, dehydration, and P—N linkage. Angew Chemie Int Ed English 1975;14:801–11.
[26] Castro BR. Replacement of alcoholic hydroxyl groups by halogens and other nucleophiles via oxyphosphonium intermediates. Org React 2004;29:1–162.
[27] Slagle JD, Huang T, Franzus B. Mechanism of the triphenylphosphine-tetrachloromethane-alcohol reaction: pericyclic or clustered ion pairs? J Org Chem 1981;46:3526–30.
[28] Standards I. ISO 4049 Dentistry—polymer based restorative materials. Int Organ Stand 2009;4:1–28.
[29] Abdallah BM, Jafari A, Zaher W, Qiu W, Kassem M. Skeletal (stromal) stem cells: an update on intracellular signaling pathways controlling osteoblast differentiation. Bone 2015;70:28–36.
[30] Al-Nbaheen M, Vishnubalaji R, Ali D, Bouslimi A, Al-Jassir F, Megges M, et al. Human stromal (mesenchymal) stem cells from bone marrow, adipose tissue and skin exhibit differences in molecular phenotype and differentiation potential. Stem Cell Rev 2013;9:32–43.
[31] Elsafadi M, Manikandan M, Atteya M, Hashmi JA, Iqbal Z, Aldahmash A, et al. Characterization of cellular and molecular heterogeneity of bone marrow stromal cells. Stem Cells Int 2016;2016.
[32] Alfotawi R, Naudi K, Dalby MJ, Tanner KE, McMahon JD, Ayoub A. Assessment of cellular viability on calcium sulphate/hydroxyapatite injectable scaffolds. J Tissue Eng 2013;4:2041731413509645.
[33] Srivastava R, Wolska J, Walkowiak-Kulikowska J, Koroniak H, Sun Y. Fluorinated bis-GMA as potential monomers for dental restorative composite materials. Eur Polym J 2017;90:334–43.
[34] Pavia DL, Lampman GM, Kriz GS, Vyvyan JA. Introduction to spectroscopy. Cengage Learning; 2014.
[35] Meyerson S. Natural abundance of chlorine isotopes. Anal Chem 1961;33:964-.
[36] Koin PJ, Kilislioglu A, Zhou M, Drummond JL, Hanley L. Analysis of the degradation of a model dental composite. J Dent Res 2008;87:661–5.
[37] Jeon M, Yoo S, Kim J, Kim C, Cho B. Dental restorative composites fabricated from a novel organic matrix without an additional diluent. Biomacromolecules 2007;8: 2571–5.
[38] Melinte V, Buruiana T, Chibac A, Mares M, Aldea H, Buruiana EC. New acid BisGMA analogs for dental adhesive applications with antimicrobial activity. Dent Mater 2016;32:e314–26.
[39] Srivastava R, Liu J, He C, Sun Y. BisGMA analogues as monomers and diluents for dental restorative composite materials. Mater Sci Eng C 2018;88:25–31.
[40] Bianchi G, Muraglia A, Daga A, Corte G, Cancedda R, Quarto R. Microenvironment and stem properties of bone marrow-derived mesenchymal cells. Wound Repair Regen 2001;9:460–6.
[41] Beun S, Bailly C, Dabin A, Vreven J, Devaux J, Leloup G. Rheological properties of experimental Bis-GMA/TEGDMA flowable resin composites with various macrofiller/microfiller ratio. Dent Mater 2009;25:198–205.
[42] Lee J-H, Um C-M, Lee I-b. Rheological properties of resin composites according to variations in monomer and filler composition. Dent Mater 2006;22:515–26.
[43] Cotugno S, Larobina D, Mensitieri G, Musto P, Ragosta G. A novel spectroscopic approach to investigate transport processes in polymers: the case of water–epoxy system. Polymer 2001;42:6431–8.
[44] Gajewski VE, Pfeifer CS, Froes-Salgado NR, Boaro LC, Braga RR. Monomers used in resin composites: degree of conversion, mechanical properties and water sorption/solubility. Braz Dent J 2012;23:508–14.
[45] Pfeifer CS, Shelton ZR, Braga RR, Windmoller D, Machado JC, Stansbury JW. Characterization of dimethacrylate polymeric networks: a study of the crosslinked structure formed by monomers used in dental composites. Eur Polym J 2011;47:162–70.
[46] Ortengren U, Wellendorf H, Karlsson S, Ruyter IE. Water sorption and solubility of dental composites and identification of monomers released in an aqueous environment. J Oral Rehabil 2001;28:1106–15.
[47] Ferracane JL. Elution of leachable components from composites. J Oral Rehabil 1994;21:441–52.
[48] Sideridou I, Tserki V, Papanastasiou G. Study of water sorption, solubility and modulus of elasticity of light-cured dimethacrylate-based dental resins. Biomaterials 2003;24:655–65.
[49] Malacarne J, Carvalho RM, de Goes MF, Svizero N, Pashley DH, Tay FR, et al. Water sorption/solubility of dental adhesive resins. Dent Mater 2006;22:973–80.
[50] Nishitani Y, Yoshiyama M, Hosaka K, Tagami J, Donnelly A, Carrilho M, et al. Use of Hoy's solubility parameters to predict water sorption/solubility of experimental primers and adhesives. Eur J Oral Sci 2007;115:81–6.
[51] Ortengren U, Andersson F, Elgh U, Terselius B, Karlsson S. Influence of pH and storage time on the sorption and solubility behaviour of three composite resin materials. J Dent 2001;29:35–41.
[52] Chaves LP, Graciano FMO, Júnior OB, do Vale Pedreira APR, Manso AP, Wang L. Water interaction with dental luting cements by means of sorption and solubility. Braz Dent Sci 2013;15:29–35.
[53] Ormsby R, McNally T, O'Hare P, Burke G, Mitchell C, Dunne N. Fatigue and biocompatibility properties of a poly(methyl methacrylate) bone cement with multi-walled carbon nanotubes. Acta Biomater 2012;8:1201–12.
[54] Jager M, Wilke A. Comprehensive biocompatibility testing of a new PMMA-hA bone cement versus conventional PMMA cement in vitro. J Biomater Sci Polym Ed 2003;14:1283–98.
[55] Bhanushali M, Bagale V, Shirode A, Joshi Y, Kadam V. An in-vitro toxicity testing-a reliable alternative to toxicity testing by reduction, replacement and refinement of animals. Int J Adv Pharm Sci 2010;1.